

Energy Efficient Battery Management

Carla-Fabiana Chiasserini, *Member, IEEE*, and Ramesh R. Rao, *Senior Member, IEEE*

Abstract—A challenging aspect of mobile communications consists in exploring ways in which the available run time of terminals can be maximized. In this paper, we present a detailed electrochemical battery model and a simple stochastic model that captures the fundamental behavior of the battery. The stochastic model is then matched to the electrochemical model and used to investigate battery management techniques that may improve the energy efficiency of radio communication devices. We consider an array of electrochemical cells. Through simple scheduling algorithms, the discharge from each cell is properly shaped to optimize the charge recovery mechanism, without introducing any additional delay in supplying the required power. Then, a battery management scheme, which exploits knowledge of the cells' state of charge, is implemented to achieve a further improvement in the battery performance. In this case, the discharge demand may be delayed. Results indicate that the proposed battery management techniques improve system performance no matter which parameters values are chosen to characterize the cells' behavior.

Index Terms—Battery management, energy consumption, wireless communication systems models.

I. INTRODUCTION

AS THE POPULARITY of radio communications increases, the reliability and energy capacity of batteries becomes a critical issue. Indeed, a greater battery capacity means a longer run time of the terminals. The design of low-energy protocols and architectures must take into account battery performance, and a tractable representation of the battery behavior must be included in the model of the overall communication system. Moreover, due to the disparity in the rate of technological advance in batteries and in portable communications equipments markets, software solutions that increase the amount of energy that a battery can deliver are worth exploring.

In this paper, we present an electrochemical battery model [1] that represents the underlying electrochemical phenomena, and we introduce a stochastic battery representation that, thanks to its simplicity, can be used to develop a broad category of protocols for energy efficient communications. The stochastic model is matched to the electrochemical model for the particular case of a lithium-ion battery, and a comparison between the results obtained is shown.

We then explore ways in which the energy efficiency of mobile wireless communications can be enhanced through the use of improved energy-efficient battery management techniques.

Manuscript received January 19, 2000; revised January 23, 2001. This work was supported by the National Science Foundation under Grant CCR 9714651.

C.-F. Chiasserini is with the Dipartimento di Elettronica, Politecnico di Torino, 10129 Torino, Italy (e-mail: chiasserini@polito.it).

R. R. Rao is with the Center for Wireless Communications, University of California, San Diego, La Jolla, CA 92093-0407 USA (e-mail: rao@cw.cw.ucsd.edu).

Publisher Item Identifier S 0733-8716(01)04706-0.

In [2], the authors introduced a discharge shaping algorithm to optimize the gain obtained from the pulsed discharge of a single cell¹. Here, we consider a battery package of L cells and apply simple scheduling techniques to efficiently distribute the discharge demand among the cells. In the *delay-free* approach the power supply is provided as soon as required. By using the postulated stochastic battery model, we show that a significant improvement in battery capacity is achieved. When scheduling algorithms are used in conjunction with discharge shaping, the battery is always able to deliver its maximum available capacity even for high discharge demand rates. In this case the price to pay is an additional delay in the power supply. This approach is named *delayed delivery*.

The remainder of the paper is organized as follows. Section II introduces some background on batteries and their performance. Section III presents the electrochemical battery model and shows results for the single cell. Section IV introduces the stochastic model and shows how accurate the postulated stochastic model is compared to the electrochemical model. Section V describes the proposed delay-free and delayed delivery battery management techniques, and presents some results. Finally, Section VI concludes the paper.

II. BACKGROUND ON BATTERY PERFORMANCE

An electrochemical cell is characterized by the initial open-circuit potential (V_{OC}), i.e., the initial value of potential of the fully charged cell under no-load conditions, and the cutoff potential (V_{cut}) at which the cell is considered discharged. Two parameters are used to represent the cell capacity: the *theoretical* and the *nominal* capacity denoted by T and N , respectively. The former is based on the amount of active materials² contained in the cell and is expressed in terms of ampere-hours; it represents the maximum available capacity of a cell. The latter represents the ampere-hours obtained from a cell when it is discharged at a specific constant current to a specific cutoff potential. Both N and T vary for different kinds of cells and values of discharge current; however, N is always much less than T . To measure the cell discharge performance the *specific power (energy)* is considered, i.e., the power (energy) expressed as watt (watt-hour) per kilogram delivered by a fully charged cell at a specified current of discharge.

The ideal electrochemical cell should be able to provide a very high energy, and to handle all the desired levels of power. In practice, the energy that can be obtained from a cell is fundamentally limited by the quantity of active material contained in the cell, and greatly depends on the intensity of the discharge

¹A battery consists of one or more cells, organized in an array. Each cell consists of an anode, a cathode, and the electrolyte that separates the two electrodes.

²Chemical materials that originate electrochemical reactions within the cell.

current, the state of charge and whether the discharge is constant or pulsed.

Under constant discharge, a cell can provide a certain value of current, called the *limiting* current [3], [4]. Above this threshold, the concentration of active materials within the cell becomes nonuniform, the cell potential drops quickly below the cutoff value, and, even if the theoretical capacity of the cell has not been exhausted, the cell is considered discharged.

Under a pulsed discharge profile, the battery is able to recover charge during the interruptions of the drained current, so called *rest time periods*. During rest time periods, active materials, that have been consumed at the electrode-electrolyte interface by electrochemical reactions, are replaced by new materials that move from the electrolyte solution to the electrode through *diffusion*. The concentration gradient of active materials therefore decreases and charge is recovered [3], [5]. As shown by several experimental tests [6]–[8], this charge recovery mechanism, so-called *recovery effect*, can lead to a significant improvement in battery performance when a pulsed discharge is implemented. It is observed that [5]: 1) by using a pulsed discharge, a higher specific power can be drained from the cell for a constant delivered specific energy. In fact, by properly choosing the pulse and the idle time duration, pulses of amplitude equal to several times the limiting current value can be obtained and 2) for a fixed power level, the delivered specific energy is greater if a pulsed discharge is used. In fact, with pulsed discharge, the active materials at the electrode-electrolyte interface are partially recovered depending on the drained power and on how long the idle periods are. Ideally, the cell would be exhausted only when all the active materials in the cell have been exploited.

The benefits of pulsed discharge continue to hold if the discharge is composed of pulses superimposed on a constant background current [9], [10]. Such discharge patterns are likely in communication devices where the baseband and RF parts need a constant supply, but load changes occur whenever the system passes from the idle to the active state or the radio transceiver switches from receive to transmit mode. An application of the pulsed discharge technique and its benefits can be observed in GSM and other TDMA based systems, where a high current is needed from the battery just during the packet transmission time (e.g., 557 μ s in GSM), otherwise a value of current about ten times lower is drained [11].

The phenomenon of charge recovery that takes place under bursty or pulsed discharge conditions is, therefore, identified as a mechanism that can be exploited to enhance the battery capacity in portable communications devices. These facts suggest that in applications that can tolerate bursty transmissions, there might be an opportunity to enhance battery discharge time by controlling the instants of transmissions. In order to explore these possibilities systematically, it is imperative that we have a reasonable model for battery behavior.

III. ELECTROCHEMICAL BATTERY MODELS

Several electrochemical models can be found in the literature for different battery technologies [1], [9], [12]. These models give a detailed representation of the underlying electrochemical phenomena; they are based on PDE (partial differential equa-

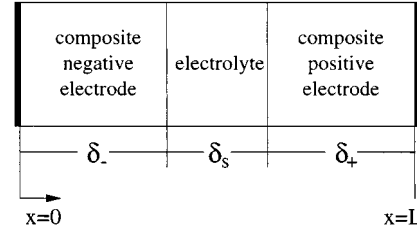


Fig. 1. Dual-insertion lithium cell consisting of composite negative and positive electrodes and electrolyte.

tion) systems and typically involve a large number of parameters that depend on the particular type of cell. The independent variables of the PDE system are the spatial coordinate x and the time t ; the dependent variables are the concentration of the chemical materials c , the drained current $I = i_1 + i_2$, and the cell potential η .

As an illustrative example, consider the model of a dual lithium ion insertion cell shown in Fig. 1, which is often used to supply portable devices. (The list of used symbols is reported in Appendix.) At the electrolyte, we have [1]

$$\frac{\partial c}{\partial t} = \frac{\partial}{\partial x} \left(D \frac{\partial c}{\partial x} \right) - \frac{i_2}{z_+ F} \frac{\partial t_+}{\partial x} \quad (1)$$

$$\frac{\partial \eta}{\partial x} = \frac{I}{k} + \frac{RT_e}{F} \left(s_+ + \frac{t_+}{z_+} \right) \frac{\partial \ln c}{\partial x}. \quad (2)$$

Equations are solved by using the boundary condition

$$-D \frac{\partial c}{\partial x} + \frac{i_2 t_+}{z_+ F} = I/F \quad \text{at } x = \delta_- \text{ for (1)} \quad (3)$$

and the initial condition $c(t = 0) = c^0$. At the cathode, we have

$$\epsilon \frac{\partial c}{\partial t} = \frac{\partial}{\partial x} \left(D \epsilon \frac{\partial c}{\partial x} \right) - \frac{i_2}{z_+ F} \frac{\partial t_+}{\partial x} + a j_n (1 - t_+) \quad (4)$$

$$\frac{\partial \eta}{\partial x} = \frac{-(I - i_2)}{\sigma} + \frac{i_2}{k} + \frac{RT_e}{F} \left(s_+ + \frac{t_+}{z_+} \right) \frac{\partial \ln c}{\partial x} \quad (5)$$

$$a j_n = \frac{-s_i}{F} \frac{\partial i_2}{\partial x} \quad (6)$$

$$\frac{\partial c}{\partial t} = D_s \left[\frac{\partial^2 c_s}{\partial r^2} + \frac{2}{r} \frac{\partial c_s}{\partial r} \right] \quad (7)$$

$$j_n = F k_2 c^{\alpha_a} (c_t - c_s)^{\alpha_a} c_s^{\alpha_c} \left[\exp \left(\frac{\alpha_a F}{RT_e} (\eta - U) \right) - \exp \left(-\frac{\alpha_c F}{RT_e} (\eta - U) \right) \right]. \quad (8)$$

The unknown variables are c in (4), η in (5), i_2 in (6), c_s in (7), and j_n in (8). The system is solved with the following boundary conditions

$$\frac{\partial c}{\partial x} = 0 \quad \text{at } x = L \text{ for (4)} \quad (9)$$

$$\frac{\partial \eta}{\partial x} = -I/\sigma \quad \text{at } x = L \text{ for (5)} \quad (10)$$

$$i_2 = I \quad \text{at } x = \delta_- \text{ and } x = \delta_- + \delta_s \text{ for (6)} \quad (11)$$

$$i_2 = 0 \quad \text{at } x = L, \quad \text{for (6)} \quad (12)$$

$$\frac{\partial c_s}{\partial r} = 0 \quad \text{at } r = 0, \quad \text{for (7)} \quad (13)$$

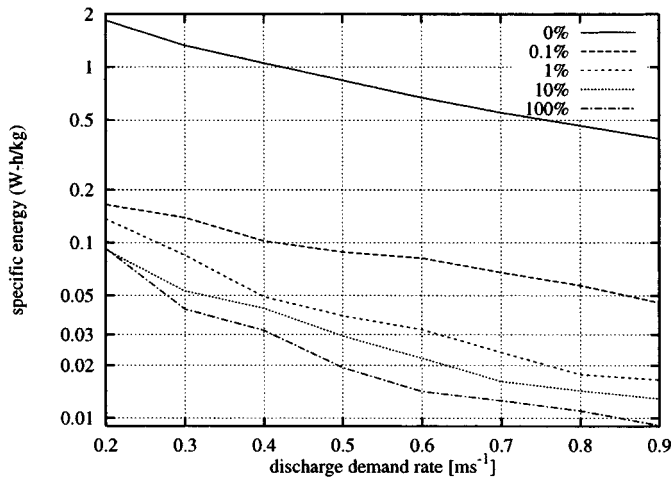


Fig. 2. Specific energy versus discharge demand rate obtained through the electrochemical model for different discharge profiles. Each profile corresponds to a different mix of 100 and 110 A/m² pulses; in the legend the percentages of 110 A/m² pulses are reported.

$$j_n = -D_s \frac{\partial c_s}{\partial r} \quad \text{at } r = R_s \text{ for (7)} \quad (14)$$

and initial conditions: $c(t = 0) = c^0$ and $c_s(t = 0) = c_s^0$. A similar system of equations can be written for the anode.

Under a stochastic discharge profile, these equations are solved by considering the current that is drained from the cell as a stochastic variable. At each current pulse, we can derive the cell potential and, hence, the energy delivered by the pulse; the discharge process ends as soon as the cell potential drops to the cutoff value.

We have obtained plots assuming that the time scale is divided into time slots with duration equal to 1 ms and that the discharge process is composed of pulses occurring at stochastic time instants according to a Bernoulli distribution. Pulses have a constant duration equal to 1 ms (i.e., equal to one time slot). The electrochemical model was numerically solved by using a program developed by Newman *et al.* [13]. The program was modified to let the discharge of the cell be driven by a stochastic process (i.e., a Bernoulli driven discharge process). Results relate to the first discharge cycle of the cell; thus, discharge always starts from a value of positive open-circuit potential equal to 4.3071 V. We assume that the cutoff potential is equal to 2.8 V, and we take the current density at each pulse as a varying parameter of the system. In practice, the cutoff potential, the pulse duration and the current density depend on the particular application (cellular phone, cordless phone, etc.) and on the technology that is used to build the electronics of the device. The values of the parameters that we consider are reasonable for the use in portable communication devices and at the same time allow us to run the program for a reasonable duration of time. Results are plotted as functions of the discharge demand rate, which is expressed as number of discharge pulses per time slot (i.e., as ms⁻¹) and coincides with the Bernoulli probability that a discharge pulse occurs in a time slot.

Fig. 2 illustrates the delivered specific energy for different discharge profiles. Each profile corresponds to a different mix of 100 and 110 A/m² pulses drained from the cell. (Labels in the plot refer to the percentages of 110 A/m² pulses.)

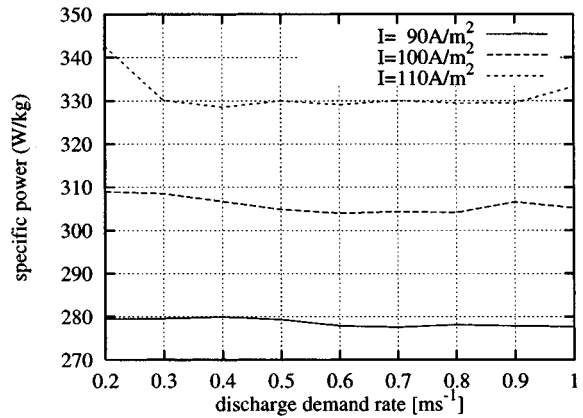


Fig. 3. Specific power versus discharge demand rate obtained through the electrochemical model for different values of current density.

Looking at the 0% and 100% curves, corresponding to 100 and 110 A/m² discharge respectively, we can see that as the discharge demand rate decreases, the obtained gain dramatically increases for both the values of current density since the chance to recover for the cell increases. This proves that a significant improvement in performance of real batteries is possible when a stochastic pulsed discharge is used.

Fig. 2 also shows that higher current density pulses may degrade performance, even if the percentage of higher current pulses is really small. This phenomenon takes place whenever the current density drained from a cell exceeds the specified limiting value and, therefore, the concentration gradient of active materials becomes significant (see Section II). The limiting current density depends on the cell technology but typically the current density required in communication systems is higher than the limiting value. Thus, applications that involve the use of different levels of power (e.g., routing in *ad hoc* networks, power control in CDMA systems, etc.) should carefully administer the available battery capacity depending on the values of drained current density and cutoff potential of the cell. It is worth noticing that for a low discharge demand rate the curves corresponding to 10% and 100% overlap since the idle time between pulses is sufficiently long for the cell to recover.

Fig. 3 presents the behavior of the specific power per pulse versus the discharge demand rate obtained from the electrochemical model as the current density varies. This plot shows that the level of specific power remains roughly constant no matter what discharge demand rate is used.

The set of results that we can derive through the electrochemical model, however, is limited because as the drained current and the cutoff potential decrease, the computation time becomes exceedingly large. In the next section, we present a more tractable parametric model that captures the essence of the recovery mechanism.

IV. STOCHASTIC BATTERY MODELS

We model the battery behavior mathematically in terms of parameters that can be related to physical characteristics of the electrochemical cell [2], [14]. The proposed stochastic model focuses on the recovery effect that is observed when a pulsed

discharge is applied, and neglects all the other phenomena represented in the electrochemical model. It is clear that when the focus is on improving the understanding of cell behavior or on cell design, a stochastic approach is not suitable and an electrochemical model must be used.

Let us consider a single cell and track the stochastic evolution of the cell from the fully charged to the completely discharged state. Models for arrays of cells can be developed from this simple cell. Discharges occur at stochastic instants determined by the discharge pattern and recovery may occur whenever there is no discharge. The amount of capacity that has to be supplied per discharge request is considered equal to c_p charge units.

Each fully charged cell is assumed to have a theoretical capacity equal to T charge units, and a nominal capacity equal to N charge units. The nominal capacity, N , is much less than T in practice and represents the charge that could be extracted using a constant discharge profile. Our ultimate goal is to extract an amount of charge that exceeds N through pulsed discharge units.

The recovery effect is modeled as a decreasing exponential function of the state of charge and discharged capacity. Such a model was used in [15], in a nonstochastic setting. To model more accurately real cell behavior [11], the exponential decay coefficient is assumed to take different values as a function of the discharged capacity.

The resulting cell behavior is a transient stochastic process that tracks the cell state of charge. The cell state of charge corresponds to the open-circuit potential of the cell, i.e., the parameter U that appeared in the electrochemical model. The stochastic process starts from the state of full charge ($V = V_{OC}$), denoted by N , and terminates when the state 0 (corresponding to a discharged cell) is reached, or the theoretical capacity T is exhausted.

Let us define q_i to be the probability that i charge units are required in one time slot, i.e., the probability that i/c_p discharge requests arrive. Thus, in each time slot, the cell has probability q_i to move from state z to $z - i$, with $0 < z \leq N$, where the positions corresponding to $z - i < 0$ add to the probability to move to 0.

During the discharge process, different phases can be identified according to the recovery capability of the cell; indeed, as charge units are drawn off, the recovery capability of the cell decreases. Let f_{\max} be the number of discharge phases that characterize the discharge process; each phase f ($f = 1, \dots, f_{\max}$) starts right after d_f charge units have been drained from the cell and ends when the number of drained charge units reaches the value d_{f+1} . We have $d_1 = 0$ and $d_{f_{\max}+1} = T$, while for d_f ($f = 2, \dots, f_{\max}$) proper values are chosen in order to match the discharge of the cell to experimental results as it will be shown in Section IV-B.

The probability to recover one charge unit in a time slot, conditioned on being in state j and phase f is

$$p_j(f) = \begin{cases} q_0 e^{-(N-j)g_N - g_C(f)} & j = 1, \dots, N-1 \\ q_1 & f = 1 \\ q_0 e^{-(N-j)g_N - d_f g_C(f)} & j = 1, \dots, N-1 \\ q_2, \dots, q_{f_{\max}} & f = 2, \dots, f_{\max} \end{cases} \quad (15)$$

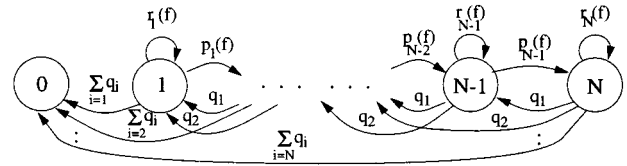


Fig. 4. Stochastic process representing the cell behavior.

where g_N and $g_C(\cdot)$ depend on the recovery capability of the battery. In particular, a small value of g_N represents a high cell conductivity, while a large g_N corresponds to a high internal resistance, i.e., a steep discharge curve for the cell. The value assumed by $g_C(\cdot)$ depends on the current phase f and is related to the cell potential drop during the discharge process, and therefore, to the discharge current I . In this way, the effect of the discharge current value on the recovery process is represented while maintaining model simplicity.

We assume that g_N is a constant, whereas $g_C(\cdot)$ is a piecewise constant function of the discharge phase; thus, it changes value in correspondence with the variable f .

The probability to remain in the same state of charge while being in phase f is

$$r_j(f) = q_0 - p_j(f) \quad j = 1, \dots, N-1 \quad (16)$$

$$r_N(f) = q_0. \quad (17)$$

A graphical representation of the stochastic process is shown in Fig. 4; a list of symbols used for the stochastic process model is reported in Appendix.

A. Performance Analysis

We assume that time is discretized into slots with unitary length and we define a *job arrival* as the event that one or more discharge requests arrive in a time slot.

The time period between the end of service of a job and the arrival of the next job at the cell is the cell rest time and is denoted by τ . When an arrival occurs, the required charge units are drained in a time slot duration. We define the cell rest time and the following time slot, where the arrival takes place, as a *cycle time*. Then, we model the discharge process of the single cell by considering just the time instants corresponding to the end of cycle times.

In each of the discharge phases the transition probabilities, $p_l(f)$ and $r_l(f)$ ($l = 1, \dots, N$; $f = 1, \dots, f_{\max}$) are constant values; we start our analysis by conditioning on the cell being in the generic phase f ($F = f$). Let us denote by $X^{(n)}$ the state of the cell at the n th cycle time. Since given $X^{(n)}$ and F , the recovery is independent of the number of charge units delivered, for $n \geq 0$ and $l = 1, \dots, N-1$ we can define

$$v_{i,j}^l(f) \triangleq P\{X^{(n+1)} = l - i, j c_p \text{ charge units delivered} \mid X^{(n)} = l, F = f\} \quad (18)$$

with $l - i > 0$ and $i \geq 0$. It can be shown that

$$v_{i,j}^l(f) = P\{\text{arrival of } j \text{ requests} \mid X^{(n)} = l, F = f\} \cdot P\{\text{recovered charge} = j c_p - i \mid X^{(n)} = l,$$

$$F = f\}. \quad (19)$$

Likewise,

$$w_j^l(f) \triangleq P\{\text{arrival of } j \text{ requests} \mid X^{(n)} = l, F = f\} \\ \cdot P\{\text{recovered charge} = jc_p \mid X^{(n)} = l, \\ F = f\} \quad (20)$$

$$z_{i,j}^l(f) \triangleq P\{\text{arrival of } j \text{ requests} \mid X^{(n)} = l, F = f\} \\ \cdot P\{\text{recovered charge} = jc_p + i \mid X^{(n)} = l, \\ F = f\} \quad (21)$$

where

$$P\{\text{arrival of } j \text{ requests} \mid X^{(n)} = l, F = f\} \\ = P\{\text{arrival of } j \text{ requests}\} = a_j. \quad (22)$$

Since the cell state of charge cannot exceed N , starting from state l a cell can recover at most $N - l$ charge units in a rest time period. The probability to recover m ($0 \leq m \leq N - l$) charge units during a rest time period, τ , can be easily derived by inspection of Fig. 4,

$$P\{\text{recovered charge} = 0 \mid X^{(n)} = l, F = f\} \\ = \sum_{k=0}^{\infty} P\{\tau = k \mid X^{(n)} = l, F = f\} r_l^k(f) \quad (23)$$

for $m > 0$,

$$P\{\text{recovered charge} = m \mid X^{(n)} = l, F = f\} \\ = \sum_{k=m}^{\infty} P\{m \text{ right transitions}, k - m \text{ transitions} \\ \text{from a state to itself} \mid \tau = k, X^{(n)} = l, F = f\} \\ \cdot P\{\tau = k \mid X^{(n)} = l, F = f\} \\ = [p_l(f) \dots p_{l+m-1}(f)] \sum_{k=m}^{\infty} \sum_{i=0}^{k-m} \sum_{j=0}^{k-m-i} \dots \sum_{v=0}^{k-m-i-j-\dots} \\ \cdot r_l^i(f) r_{l+1}^j(f) \dots r_{l+m-1}^v(f) r_{l+m}^{k-m-i-\dots-v}(f) \\ \cdot P\{\tau = k \mid X^{(n)} = l, F = f\}. \quad (24)$$

We define $u_{l,e}^{(f)}(h, n)$ as

$$u_{l,e}^{(f)}(h, n) = P\{X^{(m+n)} = e, h \text{ charge units} \\ \text{delivered} \mid X^{(m)} = l, F = f\} \quad (25)$$

with $1 \leq l \leq N$, $0 \leq e \leq N$, and $\forall m$.

It can be shown that, for $1 \leq l \leq N$, we have

$$u_{l,e}^{(f)}(h, n) = \sum_{j=1}^{\lfloor h/c_p \rfloor} \sum_{i=1}^{\min(jc_p, l-1)} v_{i,j}^l(f) u_{l-i,e}^{(f)}(h - jc_p, n - 1) \\ + \sum_{j=1}^{\lfloor h/c_p \rfloor} w_j^l(f) u_{l,e}^{(f)}(h - jc_p, n - 1)$$

$$+ \sum_{j=1}^{\lfloor h/c_p \rfloor} \sum_{i=1}^{N-l} z_{i,j}^l(f) u_{l+i,e}^{(f)}(h - jc_p, n - 1) \quad (26)$$

$$u_{1,e}^{(f)}(h, n) = \sum_{j=1}^{\lfloor h/c_p \rfloor} w_j^1(f) u_{1,e}^{(f)}(h - jc_p, n - 1) \\ + \sum_{j=1}^{\lfloor h/c_p \rfloor} \sum_{i=1}^{N-1} z_{i,j}^1(f) u_{1+i,e}^{(f)}(h - jc_p, n - 1) \quad (27)$$

$$u_{N,e}^{(f)}(h, n) = \sum_{j=1}^{\lfloor h/c_p \rfloor} \sum_{i=1}^{\min(jc_p, N-1)} a_j u_{N-i,e}^{(f)}(h - jc_p, n - 1). \quad (28)$$

Equations (26)–(28) can be solved iteratively for each possible value of h and n ($n \leq (d_{f+1} - d_f)/c_p$) with the boundary conditions

$$u_{l,e}^{(f)}(h, n) = 0 \quad \text{for } n > 1, h < c_p \text{ and } \forall l, e. \quad (29)$$

The probability that the discharge process passes from phase f to phase $f + 1$ at the end of n cycle times and having delivered h charge units, is equal to the probability to deliver $k < h$ charge units in $n - 1$ cycle times without leaving phase f , multiplied by the probability to deliver $h - k$ charge units during the last cycle time. Clearly, this can be easily computed once we solve (26)–(28).

At this point, we can derive the average number of charge units, A_{cu} , drained from a cell during the discharge process. For the sake of simplicity, let us consider just two phases of discharge ($f = 1, 2$). Three different events may occur: 1) the discharge process ends in the state 0 after n cycle times while being in phase $f = 1$ and having delivered h ($h \leq T$) charge units; 2) the discharge process ends in the state 0 after n cycle times while being in phase $f = 2$ and having delivered h ($h \leq T$) charge units; or 3) T charge units are delivered after n cycle times without having the process reached state 0.

Since the cell is assumed to be in phase 1 and state N at the beginning of the discharge process, the probabilities of the three events are

$$P\{X^{(n)} = 0, h \text{ units delivered, charge delivered in} \\ F = 1 \mid X^{(0)} = N, F^{(0)} = 1\} \\ = \begin{cases} u_{N,0}^{(1)}(h, n), & \text{if } h \leq d_1 \text{ or } n = 1 \\ \sum_{k=1}^{d_1-1} \sum_{s=1}^N u_{N,s}^{(1)}(k, n - 1) u_{s,0}^{(1)}(h - k, 1), & \text{if } h > d_1 \text{ and } n > 1 \end{cases} \quad (30)$$

where the first equation holds when phase 1 is never crossed, while the second equation holds when phase 1 is crossed during the n th cycle time

$$P\{X^{(n)} = 0, h \text{ units delivered, charge delivered in} \\ F = 1, 2 \mid X^{(0)} = N, F^{(0)} = 1\} \\ \cdot \sum_m \sum_{t=1}^N \sum_{s=1}^N \sum_{k=d_1}^{h-1} \sum_{j=1}^{d_1-1} u_{N,s}^{(1)}(j, m - 1) u_{s,t}^{(1)}(k - j, 1)$$

$$\cdot u_{t,0}^{(1)}(h-k, n-m) \quad (31)$$

where j charge units are delivered in phase 1, $k-j$ while crossing phase 1, and $h-k$ in phase 2 ($\forall j, k$)

$$\begin{aligned} & P\{X^{(n)} > 0, T \text{ units delivered} | X^{(0)} = N, F^{(0)} = 1\} \\ &= \sum_{e=1}^N \left[\sum_{s=1}^N \sum_{k=1}^{d_1-1} u_{N,s}^{(1)}(k, n-1) u_{s,e}^{(1)}(T-k, 1) \right. \\ &+ \sum_m^N \sum_{t=1}^N \sum_{s=1}^N \sum_{k=d_1}^{T-1} \sum_{j=1}^{d_1-1} u_{N,s}^{(1)}(j, m-1) u_{s,t}^{(0)}(k-j, 1) \\ &\left. \cdot u_{t,e}^{(2)}(T-k, n-m) \right] \quad (32) \end{aligned}$$

where the first term is the probability that k ($\forall k < d_1$) charge units are delivered in $n-1$ cycle times and $T-k$ in the n th cycle time; the second term is the probability that j charge units are delivered while being in phase 0, $k-j$ while crossing phase 1, and the remaining $T-k$ during phase 2 ($\forall j, k$).

Thus, we have

$$\begin{aligned} A_{cu} = & \sum_n \left(\sum_{h=1}^T h \cdot P\{X^{(n)} = 0, h, \text{ charge delivered in} \right. \\ & F = 1 | X^{(0)} = N, F^{(0)} = 1\} \\ & + \sum_{h=d_1+1}^T h \cdot P\{X^{(n)} = 0, h, \text{ charge delivered in} \\ & F = 1, 2 | X^{(0)} = N, F^{(0)} = 1\} \\ & \left. + T \cdot P\{X^{(n)} > 0, T | X^{(0)} = N, F^{(0)} = 1\} \right) \quad (33) \end{aligned}$$

The mean number of discharge requests that have been served, A_p , results as the ratio of the average number of charge units drained from the cell to the number of charge units delivered per discharge request: $A_p = A_{cu}/c_p$.

We consider as a performance index the ratio of A_p to the number of discharge requests that can be served by the cell under constant current discharge, we have

$$G = (A_p \cdot c_p)/N = A_{cu}/N. \quad (34)$$

Notice that G represents the capacity gain that is obtained from the discharge process with respect to the cell nominal capacity; greater G is, higher the delivered capacity. However, since the delivered capacity can not exceed the theoretical capacity, G can be at most equal to T/N .

B. Validation of the Stochastic Model

In this section, we present a comparison between results obtained through the electrochemical model of the dual lithium ion insertion cell and those derived from the stochastic model. The discharge demand is assumed to be a Bernoulli-driven stochastic process.

Results obtained from the stochastic model are derived under the following assumptions: $c_p = 1$, $f_{\max} = 3$, N equal to the number of pulses obtained through the electrochemical model

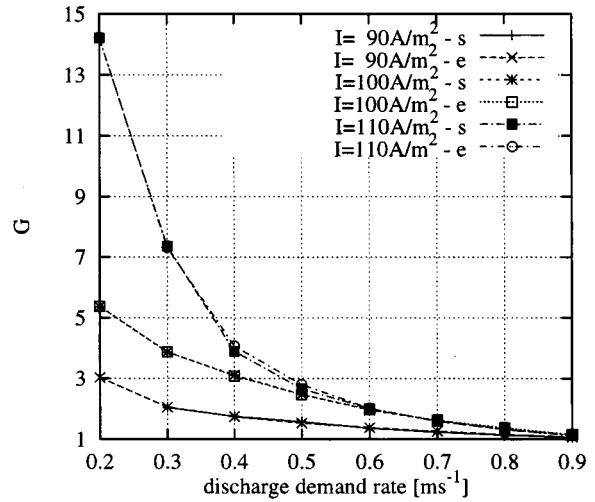


Fig. 5. Gain obtained under pulsed discharge with respect to constant discharge for different values of drained current density. Results derived by using the electrochemical (e) and the stochastic (s) model are compared.

under constant discharge, and T equal to the number of pulses obtained through the electrochemical model under a discharge demand rate equal to 0.1.

Fig. 5 presents the behavior of G versus the rate at which the current pulses are drained for three values of current density: $I = 90, 100, \text{ and } 110 \text{ A/m}^2$. As it can be seen, the curves obtained from the electrochemical and the stochastic models match closely.

The procedure to fit the two sets of curves is straightforward. Indeed, looking at the results obtained through the electrochemical model, we can identify for each curve about three regions as the discharge demand rate varies. Notice that the number of regions is related to the number of discharge phases, that can be set up equal to 3 for most cell technologies. In each region, the curve is well approximated by an exponential function with a certain parameter. Therefore, to fit the curves obtained through the electrochemical and the stochastic frameworks, we take $g_N = 0$ and vary the parameters g_C and d_f ($f = 2, \dots, f_{\max}$) of the stochastic model according to the considered value of current density. Following this procedure, we obtain a maximum error equal to 4% and an average error equal to 1%.

Fig. 6 shows the same curves derived from the electrochemical model and from a simplified version of the stochastic model. The simplified stochastic representation of the cell is obtained by considering the parameter g_C to be independent of the discharged capacity. In particular, here g_C is a constant value equal to: $(1/d_{f_{\max}}) \sum_{f=1}^{f_{\max}-1} g_C(d_f)(d_{f+1} - d_f)$. In this case, we have a maximum error equal to 44% and an average error equal to 14% for $I = 110 \text{ A/m}^2$, and a maximum error equal to 14% and an average error equal to 5% for $I = 90 \text{ and } 100 \text{ A/m}^2$.

We point out that the validation of the stochastic model through the dual lithium ion insertion cell was a natural choice since lithium-based batteries are widely used in portable devices and also because of the availability of the program developed by Newman *et al.* [13] that models this cell. However, a validation of the stochastic model for other cell technologies can be done by considering proper PDE electrochemical models [9], [12]. Once we have the electrochemical model

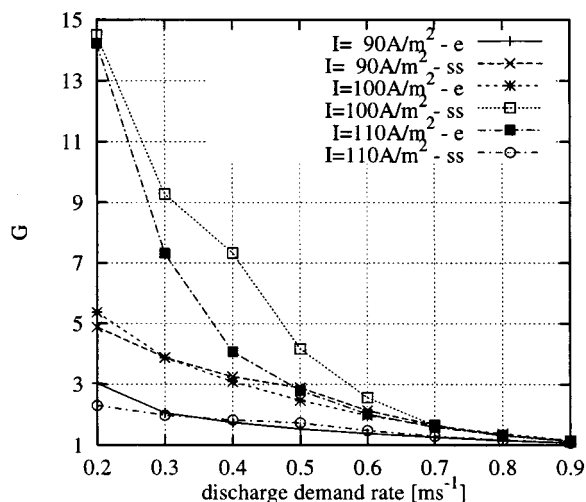


Fig. 6. Gain obtained under pulsed discharge with respect to constant discharge for different values of drained current density. Results derived by using the electrochemical (e) and the simplified stochastic (ss) model are compared.

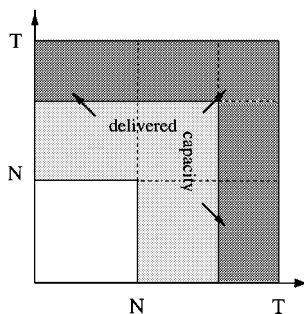


Fig. 7. Margin of improvement for the capacity delivered by an array of $L = 2$ cells.

for the considered cell technology, curves representing G as a function of the discharge demand rate can be derived. The parameters of the stochastic model are set up following the procedure described above.

V. BATTERY MANAGEMENT TECHNIQUES

In this section, we use the presented stochastic battery model to explore ways in which the energy efficiency of mobile wireless communications can be enhanced through the use of improved energy-efficient battery management techniques.

We consider a battery package of L cells that can be selectively scheduled. Fig. 7 illustrates the case for $L = 2$. A capacity equal to N can be drained from each cell by means of a constant current discharge. However, by using a proper pulsed discharge technique, the region of delivered capacity can be increased. Our goal is to find methods to extend the region of delivered capacity up to the maximum limit (T). Indeed, in the presence of bursty data traffic, we may be able to adjust traffic arrivals and battery discharge profile so that the recovery mechanism can be fully exploited.

We first review some results related to *load balancing* that are close to our problem. Then, we apply the load balancing algorithms to battery management. We consider both a *delay-free*

and *delayed delivery* approach. The former implements a scheduling scheme among the cells and provides the power supply as soon as required; the latter uses scheduling algorithms in conjunction with discharge shaping, so that an additional delay is introduced in the power supply.

A. Related Work on Load Balancing

Load balancing algorithms are classified as static or dynamic depending on whether they depend on the current state of the system nodes. Dynamic load balancing policies improve load distribution at the expense of additional communication of the system status and processing overhead. Static algorithms have better performance when the system load is light to moderate or when the cost of the communication among the nodes is high.

In [16], it is proved that the shortest queue (SQ) policy maximizes the system performance if queues have infinite capacities and the service time distributions are exponential; in [17], it is proved that the SQ policy is optimal for a broader class of service time distributions, i.e., *increasing with likelihood ratio* distributions. However, the SQ scheme seems more suitable for centralized systems, while for distributed systems randomized load balancing schemes are well applicable.

Static randomized algorithms have been studied in [18] where Karp *et al.* show that two hash functions instead of one provide an exponential improvement in the maximum load of a hash bucket.

In [19] and [20], dynamic randomized schemes are considered. The *supermarket* model is analyzed and an important result is derived. In this model, customers arrive as a Poisson process at n servers; each customer chooses d servers at random from the n servers and waits for service at the one with the shortest queue. It is shown that using $d = 2$ choices yields an exponential improvement in the customer's mean waiting time over the case $d = 1$. Also it is shown that for $d > 2$ no significant improvements accrue relative to $d = 2$. Then, to reduce the number of choices (i.e., the cost of the scheme), *threshold models* are examined. In this case, a customer can make a second choice only if the load at the first server exceeds a certain threshold.

B. A Delay-Free Approach

Similarly to load balancing, the objective here is to find a scheduling policy that efficiently distributes the discharge demand among cells connected in parallel.

We first apply to the cell array two different static policies, i.e., policies that are independent of the cells state of charge, and we compare their performances. We assume that the battery discharge demand is driven by Poisson-distributed requests arrivals with rate R , at each time slot the probability that i discharge requests arrive is: $a_i = (R^i e^{-R} / i!)$ $i \geq 0$, and the probability that the job inter-arrival time is equal to k time slots is geometrically distributed

$$P\{\text{inter arrival time} = k\} = e^{-R(k-1)}(1 - e^{-R}). \quad (35)$$

Also, we assume that at each job arrival the time necessary to drain the required current supply is always equal to one time slot.

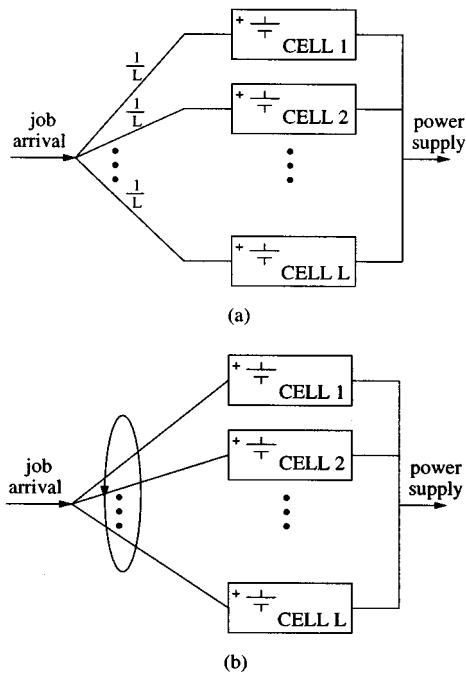


Fig. 8. Scheduling algorithms applied to the cells discharge. (a) Random (RD). (b) Round robin (RR).

The first technique that we consider is a random scheme, indicated by RD, such that a job arrival is directed to each of the L cells with probability equal to $1/L$, regardless of the number of discharge requests constituting the job. The discharge request arrival process at each cell is still Poisson but with rate equal to R/L . A graphical representation of the RD scheme is given in Fig. 8(a).

The second technique is the round robin (RR) scheduling shown in Fig. 8(b). The job arrivals are directed to the cells by switching from a cell to the next one. In this case, the distribution of the job interarrival times is derived by convolving L probability functions, whose expression is written in (35). For $L = 2$, we have

$$P\{\text{inter arrival time} = k\} = (k-1)e^{-R(k-2)}(1 - e^{-R})^2. \quad (36)$$

The behavior of the capacity gain G is derived for delay-free schemes as a function of the average discharge request arrival rate R . We assume $N = 25$, $c_p = L = 2$, and $f_{\max} = 3$.

Fig. 9 shows analytical results obtained for two different values of g_N . Clearly, for both the RD and the RR schemes the gain that we obtain increases as g_N decreases, i.e., as the charge recovery capability of the cells improves. However, since the rest time duration under the RR technique is always twice the rest time that a single cell would experience, the RR outperforms the random scheme.

The performance of a modified RR algorithm, that operates taking into account the cell state of charge in the job assignment to the cells, has been derived by simulation. We call this scheme the *best-of-two* (BT) policy since it is close to the dynamic load balancing method where customers choose the best of $d = 2$ servers randomly chosen. As we can see looking at Fig. 9, an improvement is obtained in the behavior of G with respect to

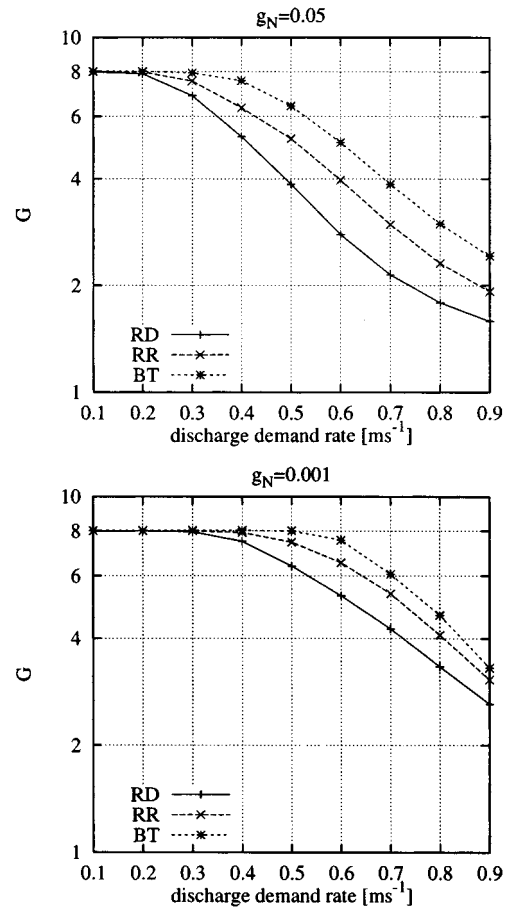


Fig. 9. Gain obtained applying different discharge techniques for $L = 2$, $N = 25$, $T = 200$, and g_N varying. RD = random; RR = round robin; BT = best-of-two.

the results presented for the RR method, especially when $g_N = 0.05$. However, every time a cell is drained (i.e., a service is required), the state of the server changes; therefore, we need to monitor and compare the cells status whenever we have to assign a job to a cell. The discharged capacity of the cells can be tracked thanks to smart battery packages [21] but the system complexity may increase significantly and the delay due to the overhead may not be negligible.

We conclude that an efficient way to discharge a battery is to guarantee to each cell a rest time long enough to recover. A relevant performance improvement is achieved by adopting a simple round robin technique and this improvement is evident no matter which values for the cells parameters are considered.

C. A Delayed Delivery Approach

Here, we consider battery management techniques that involve a coordination among the cells of the array and drain current from the cells according to their state of charge.

Our goal is to monitor the cells status and make them recover as much as they need to obtain the maximum available capacity from the discharge process.

We define a lower threshold for the cell state of charge such that whenever the state of charge drops to this value, the cell is considered *not active* and current cannot be drawn off until recovery occurs. The event of the cell state of charge dropping to

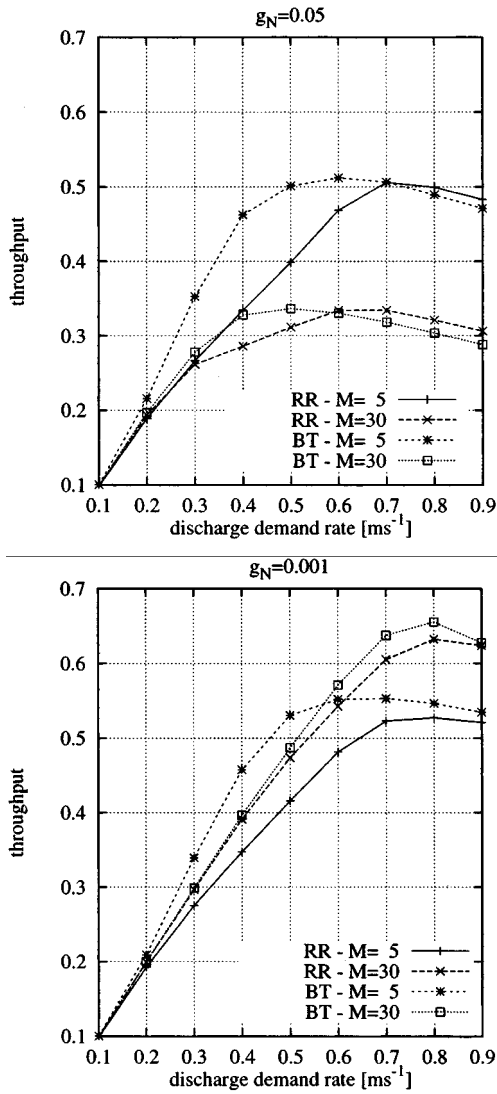


Fig. 10. Throughput obtained using the proposed delayed delivery techniques. $L = 2, T = 200, g_N = 0.05$ and M varying. RR = round robin; BT=best-of-two.

a certain threshold can be easily revealed by the control apparatus present in smart battery packages; the acquisition of the information is, therefore, considered instantaneous.

Among the set of active cells, the RR and the BT schemes are applied as described in Section V-B. Whenever the state of charge of a cell drops to the value of threshold, the cell is removed from the set of active cells and allowed to recover. If none of the cells is active, the discharge requests that arrive are buffered and served as soon as a sufficient amount of charge is recovered. We also assume that if a cell becomes inactive while serving a discharge request, the remaining necessary charge is drained from the next active cell.

As the discharged capacity becomes close to the value of theoretical capacity, the adopted scheme is suspended and cells are discharged as long as their voltage drops to the cutoff value.

In this scheme, an important parameter for the cell behavior is the difference between the initial value of charge, N , and the charge threshold that is chosen. We denote this quantity by M .

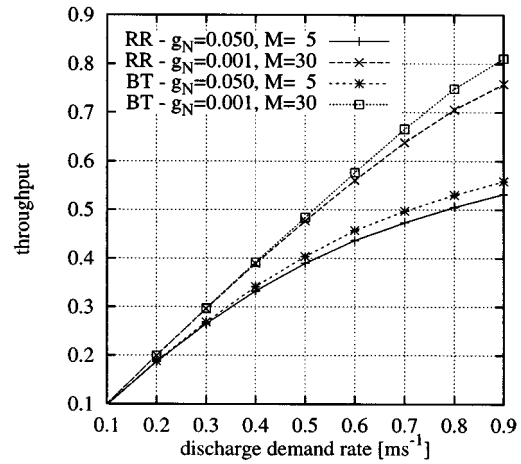


Fig. 11. Throughput obtained using the proposed delayed delivery techniques. $L = 2, T = 200, g_N = 0.001$ and M varying. RR = round robin; BT = best-of-two.

Results obtained by simulation are presented in Figs. 10–11 for $c_p = L = 2, f_{max} = 3, T = 200$ and M varying. We derive the throughput, computed as the ratio of the number of discharge requests that have been served to the discharge process duration. Note that here the capacity gain G , previously considered, is always equal to T/N , that is its maximum value, since the introduced delay is sufficient to let the cell recover all the available charge.

Curves in Figs. 10 and 11 are obtained for $g_N = 0.05$ and $g_N = 0.001$, respectively. For $g_N = 0.05$ and both the RR and BT schemes, performance improves as smaller values of M are considered. However, for any value of M , the throughput decreases. This is because, as soon as the discharge process starts, the cell quickly reaches the value of the threshold, that is far away from the initial charge. At this point, the recovery probability is low and the delay before being able to resume the discharge process becomes large; thus, the time period needed to drain from the cell the total number of available charge units increases. When this phenomenon takes place, we have to reduce the cell load by using a larger array of cells so that we move to the more favorable region of operation. Also, we note that when we are in the region where the battery operates correctly (i.e., the discharge demand rate is less than 0.6) the BT policy outperforms the RR scheme. However, we recall that the improvement in performance presented by the BT algorithm must be balanced with the increased system complexity. Note that, in this study, we considered the time necessary to compare the cells status to be negligible.

For $g_N = 0.001$, the results shown in Fig. 11 present a much higher throughput since the recovery capability of the cells is much superior. In this case, larger values of M give better performance since now cells are able to quickly recover even when their state of charge is greatly reduced relative to the initial value. The BT gives the best performance for any value of the discharge demand rate; however, we still notice that for both the schemes the throughput starts decreasing at a certain point.

In Fig. 12, we presents the same curves obtained with $L = 4$, and considering $M = 5$ for $g_N = 0.05$ and $M = 30$ for

$g_N = 0.001$. As expected, in this case the throughput always increases as the discharge demand rate grows.

The proposed battery management techniques provide a significant gain in performance and this is achieved with a reasonably small additional delay in the discharge demand supply for all values of the considered cell parameters. The improvement relative to a simple round robin scheme is evident; however, in this case a smart battery package has to be used and greater complexity is involved.

VI. CONCLUSION

In this paper, we presented a stochastic battery model that closely matches results obtained through an electrochemical model. Thanks to its simplicity, the postulated model can be used for the design of low-power communication systems and energy aware communication protocols.

We used the stochastic model to explore battery management techniques that improve the battery capacity and, therefore, the run time of communications devices. A battery package composed of an array of cells was considered. The combination of the charge recovery mechanism with discharge management techniques applied to the cells array showed an increase in the battery performance.

Analytical results indicated that performance can be significantly increased without introducing any delay in the discharge demand supply by implementing a round robin scheme. Moreover, it was shown by simulation that a battery is able to deliver the maximum available capacity at the cost of a fairly small additional delay and complexity when scheduling is combined with a simple discharge shaping technique.

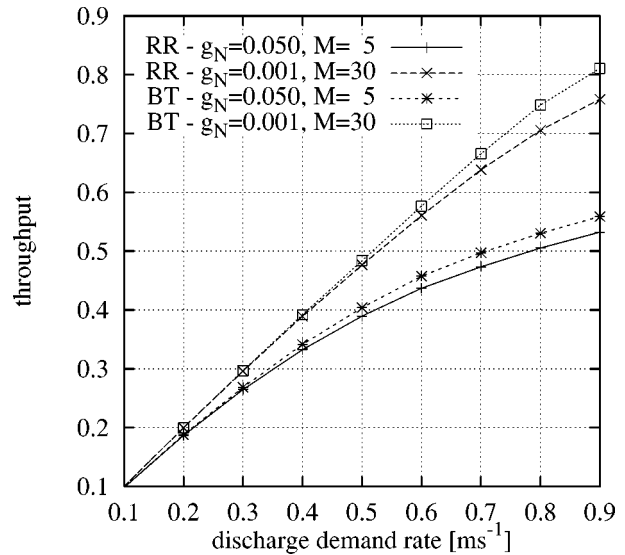


Fig. 12. Throughput obtained using the proposed delayed delivery techniques. $L = 4$, $T = 200$, and g_N varying. RR = round robin; BT = best-of-two.

APPENDIX I LIST OF ACRONYMS

BT	Best-of-two.
CDMA	Code division multiple access.
GSM	Global system mobile communications.
PDE	Partial differential equation.
RD	Random.
RF	Radio frequency.
RR	Round robin.
SQ	Shortest queue.
TDMA	Time division multiple access.

APPENDIX II LIST OF SYMBOLS

Electrochemical Battery Model.	
i_1	Electronic current density (A/m ²).
i_2	Ionic current density (A/m ²).
I	Superficial current density (A/m ²); $I = i_1 + i_2$.
j_n	Pore-wall flux across interface between electrolyte and electrode (mol/m ² /s).
η	Difference between the cathode potential and the electrolyte potential (V).
U	Open-circuit potential (V).
c	Concentration of electrolyte in the electrolyte.
c_s	Concentration of the active material in the solid matrix.
t_+	Transference number of the positive active material.
F	Faraday's constant (96,487 C/eq).
R	Universal gas constant (8.3143 J/mol/K).
T_e	Temperature (298.15 K).
k	Conductivity of the electrolyte (S/m).
σ	Conductivity of solid matrix (S/m).
z_+	Charge number.
s_i	Stoichiometric coefficient of active material i in the electrode reaction.
a	Specific interfacial area (m ⁻¹).

R_s	Radius of cathode material (μm).
ϵ	Porosity of the cathode.
D	Diffusion coefficient of electrolyte, (m^2/s).
D_s	Diffusion coefficient of lithium in the solid matrix (m^2/s).
δ_s	Thickness of the electrolyte ($50 \mu\text{m}$).
δ_+	Thickness of the composite positive electrode (μm).
δ_-	Thickness of the composite negative electrode (μm).
L	Thickness of the cell; $L = \delta_- + \delta_s + \delta_+$.
k_2	Reaction rate constant at cathode/electrolyte interface ($\text{m}^4/\text{mol}/\text{s}$).
c_t	Maximum concentration in solid (mol/m^3).
α_a, α_c	Transfer coefficients.
Stochastic Battery Model.	
c_p	Amount of capacity that has to be supplied per discharge request.
T	Theoretical capacity of the cell.
N	Nominal capacity of the cell.
q_i	Probability that i charge units are required in one time slot.
f_{\max}	Number of discharge phases.
d_f	Duration of discharge phase f , expressed as
$d_{f+1} - d_f$	number of drained charge units.
g_N	Exponential decay coefficient; it is related to cell conductivity.
g_C	Exponential decay coefficient; it is related to cell potential drop during the discharge phase.
$p_j(f)$	Probability to recover one charge unit in one time slot, conditioned on being in state j and phase f .
$r_j(f)$	Probability to remain in the same state of charge, conditioned on being in state j and phase f .

REFERENCES

[1] M. Doyle, T. F. Fuller, and J. S. Newman, "Modeling of galvanostatic charge and discharge of the lithium/polymer/insertion cell," *J. Electrochem. Soc.*, vol. 140, pp. 1526–1533, June 1993.

[2] C. F. Chiasserini and R. R. Rao, "A traffic control scheme to optimize the battery pulsed discharge," in *Proc. Milcom*, Atlantic City, NJ, Nov. 1999.

[3] H. D. Linden, *Handbook of Batteries*, 2nd ed. New York: McGraw-Hill, 1995.

[4] M. Doyle and J. S. Newman, "Analysis of capacity-rate data for lithium batteries using simplified models of the discharge process," *J. Applied Electrochem.*, vol. 27, no. 7, pp. 846–856, July 1997.

[5] C. F. Chiasserini and R. R. Rao, "Pulsed battery discharge in communication devices," in *Proc. MobiCom*, Seattle, WA, Aug. 1999.

[6] T. F. Fuller, M. Doyle, and J. S. Newman, "Relaxation phenomena in lithium-ion-insertion cells," *J. Electrochem. Soc.*, vol. 141, no. 4, pp. 982–990, Apr. 1994.

[7] R. M. LaFollette, "Design and performance of high specific power, pulsed discharge, bipolar lead acid batteries," in *10th Annu. Battery Conf. Applications and Advances*, Long Beach, CA, Jan. 1995, pp. 43–47.

[8] B. Nelson, R. Rinehart, and S. Varley, "Ultrafast pulse discharge and recharge capabilities of thin-metal film battery technology," in *11th IEEE Int. Pulsed Power Conf.*, Baltimore, MD, June 1997, pp. 636–641.

[9] R. M. LaFollette and D. Bennion, "Design fundamentals of high power density, pulsed discharge, lead-acid batteries. II Modeling," *J. Electrochem. Soc.*, vol. 137, no. 12, pp. 3701–3707, Dec. 1990.

[10] B. Le Pioufle, J. F. Fauvarque, and P. Delalande, "Comportement non linéaire des générateurs électrochimiques associés aux convertisseurs statiques. Détection de l'état de charge" (in French), *Eur. Phys. J. Appl. Phys.*, vol. 2, no. 3, pp. 257–265, June 1998.

[11] Tadiran Electronic Industries. Make the right battery choice for portables. [Online]. Available: <http://www.tadiranbat.com/howrchg.htm>.

[12] R. M. LaFollette and J. N. Harb, "Mathematical model of the discharge behavior of a spirally wound lead-acid cell," *J. Electrochem. Soc.*, vol. 146, no. 3, pp. 809–818, Mar. 1999.

[13] J. S. Newman. (1999, July) FORTRAN Programs for Simulation of Electrochemical Systems. [Online]. Available: <http://www.cchem.berkeley.edu/~jsngrp/>.

[14] C. F. Chiasserini and R. R. Rao, "Energy efficient battery management," in *Proc. Infocom*, Tel Aviv, Israel, Mar. 2000, pp. 396–403.

[15] J. Alzieu, H. Smimite, and C. Glaize, "Improvement of intelligent battery controller: State-of-charge indicator and associated functions," *J. Power Source*, vol. 67, no. 1, pp. 157–161, July 1997.

[16] A. Ephremides, P. Varaiya, and J. Walrand, "A simple dynamic routing problem," *IEEE Trans. Automat. Contr.*, vol. 25, pp. 69–693, Aug. 1980.

[17] G. Koole, P. Sparaggis, and D. Towsley, "Minimizing response times and queue lengths in systems of parallel queues," *J. Appl. Probability*, vol. 56, pp. 1185–1193, Dec. 1999, to be published.

[18] R. M. Karp, M. Luby, and F. Meyer aud der Heide, "Efficient PRAM simulation on a distributed memory machine," in *Proc. 24th ACM Symp. Theory of Computing*, Victoria, BC, Canada, May 1992, pp. 318–326.

[19] M. Mitzenmacher, "On the analysis of randomized load balancing schemes," *Theor. Comput. Syst.*, vol. 32, no. 3, pp. 361–386, May 1999.

[20] D. L. Eager, E. D. Lazokwska, and J. Zahorjan, "Adaptive load sharing in homogeneous distributed systems," *IEEE Trans. Software Eng.*, vol. SE-12, pp. 662–675, May 1986.

[21] Cadex Electronics Inc. Intelligent batteries. [Online]. Available: <http://www.cadex.com/cfm/index>.



Carla-Fabiana Chiasserini (S'98–M'00) received the Laurea degree in electrical engineering from University of Florence, Italy, in 1996, and the Ph.D. degree from Politecnico di Torino, Italy, in 1999. She is currently with the Department of Electrical Engineering, Politecnico di Torino, as an Assistant Professor. She was with the Center for Wireless Communications, University of California, San Diego, as a Visiting Researcher in 1999 and 2000. Her research interests include architectures, protocols, and performance analysis of wireless networks.

Ramesh R. Rao (M'85–SM'90) received the Bachelor's degree (with honors) in electrical and electronics engineering from the University of Madras, India, in 1980. He received the MS degree in 1982 and the Ph.D. degree in 1984 from the University of Maryland, College Park, Maryland. Since 1984, he has been with the Faculty of the Department of Electrical and Computer Engineering, the University of California, San Diego, where he is currently Professor and Director of the Center for Wireless Communications. His research interests include architectures, protocols, and performance analysis of wireless, wireline, and photonic networks for integrated multimedia services. Dr. Rao has served as the Editor of the Information Theory Society Newsletter from 1993 to 1995 and is the founding Web Editor of the Information Theory Society web site. He was elected to the IEEE Information Theory Society Board of Governors in 1997 and 2000. He is the Editor for Packet Multiple Access of the IEEE TRANSACTIONS ON COMMUNICATIONS and is a member of the Editorial Board of the ACM/Baltzer Wireless Network Journal as well as IEEE Network magazine. He has been a Guest Editor for special issues of several ACM and IEEE journals. He regularly serves as a member of the Technical Program Committees of IEEE conferences and as a reviewer for agencies such as the National Science Foundation.